High Spatial Resolution Imaging of a Supersonic Underexpanded Jet Impinging on a Flat Plate

Buchmann, N. A.; Mitchell, D. M.; Ingvorsen, Kristian Mark; Honnery, D. R.; Soria, J.

Publication date:
2011

Document Version
Publisher's PDF, also known as Version of record

Citation (APA):
Buchmann, N. A., Mitchell, D. M., Ingvorsen, K. M., Honnery, D. R., & Soria, J. (2011). High Spatial Resolution Imaging of a Supersonic Underexpanded Jet Impinging on a Flat Plate. Abstract from 6th Australian Conference on Laser Diagnostics in Fluid Mechanics and Combustion, Canberra, Australia.

High Spatial Resolution Imaging of a Supersonic Underexpanded Jet Impinging on a Flat Plate

N. A. Buchmann[1], D. M. Mitchell[1], K. M. Ingvorsen, D. R. Honnery[1] and J. Soria[1]

[1]Department of Mechanical and Aerospace Engineering, Monash University, VIC 3800, AUSTRALIA
nicolas.buchmann@monash.edu

[2]Department of Mechanical Engineering, Technical University of Denmark, DK-2800 Kgs. Lyngby, Denmark

ABSTRACT

High spatial resolution Schlieren imaging is used to characterize the instantaneous flow structure of a normally impinging supersonic, underexpanded jet, which plays an important role in aerospace and manufacturing application such as cold spray coating processes. The Z-type Schlieren systems consist of a high-resolution CCD camera operated at $1000 fps$ and a pulsed high-power LED for illumination. Visualisations of the axial and radial density gradient are presented for a nozzle pressure ratio of NPR = 3.2 and a jet stand-off distance of $z/D = 4$. The presented high-resolution visualizations clearly demonstrate the acoustic feedback-loop in which shear-layer instabilities are amplified under the influence of upstream traveling acoustic waves to cause the growth of large-scale, Kelvin-Helmholtz like structures. Further evidence of these instabilities and their interaction with the acoustic field is given by the two-point-correlation of the axial density gradient.

1. INTRODUCTION

Supersonic, underexpanded jets play an important role in a range of aerospace and manufacturing applications. For example, in aerospace this type of flow is commonly found in short takeoff and vertical landing aircraft an spacecraft and rocket launches. In the manufacturing industry, supersonic underexpanded jets are typical for a process referred to as cold gas-dynamic spray coating. Cold gas-dynamic spray coating is a spray process wherein small particles (typically several μm) in solid state, are accelerated to supersonic velocities and upon impaction against a substrate form a deposit or coating.

Underexpanded jets form when the exit is greater than that of the atmosphere surrounding the jet. In these situation the pressure in the jet is equalised with the atmospheric pressure through a series of shock cells and shock waves. The flow phenomena associated with underexpanded free jets have been investigated extensively in the past (Donaldson and Snedeker, 1971; Carling and Hunt, 1977; Henderson et al., 2005) and their steady-state structure is relatively well understood.
A different situation however arises when the fluid jet impinges on a perpendicular surface. Naturally, underexpanded jets exhibit instabilities in the shear-layer that forms between the nozzle lip and the sonic flow exiting the nozzle as can be seen for example in Figure 3. The interaction of the jet with the impingement surface causes coherent pressure fluctuations, which generate acoustic waves that travel upstream towards the jet nozzle. Certain combinations of pressure ratio, impingement angle and distance from the surface lead to an amplification of the shear-layer instabilities, effectively creating a closed-loop excitation mechanism. The existence of such feedback mechanisms has been previously studied experimentally by Krothapalli et al. (1999); Henderson et al. (2005) and Risborg et al. (2008). As the phenomena responsible for these instabilities occur at very small spatial and temporal scales their study requires instantaneous, high-resolution measurement techniques such as high-speed Schlieren and/or Shadowgraphy.

These instabilities and the jet oscillations thereof are related to some fundamental problems currently encountered in cold spray coating. As these processes heavily rely on the injection and acceleration of solid particles into the supersonic gas jet, it is important to obtain a fundamental understanding on how the flow field affects the trajectory, impingement velocity and impingement angle of these particles. Hence, as a first step the motivation of the present study is to gain a better understanding of the dynamic jet structure of the underexpanded impinging jet. For this purpose high spatial resolution Schlieren measurements are conducted of a normally impinging jet at a fixed stand-off distance and nozzle pressure ratio.

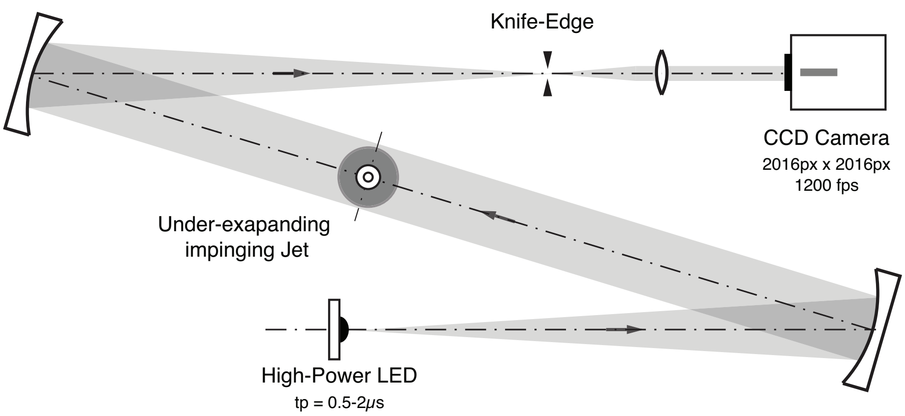

Figure 1: High resolution Z-type Schlieren setup with pulsed high-power LED illumination.

2. EXPERIMENTAL METHODOLOGY

The supersonic, underexpanded jet is created by a 15*mm* converging nozzle operated at a continuous supply pressure of compressed air up to 700*kPa*. The parameters characterising the super-sonic impinging jet are the nozzle pressure ratio (NPR) and the stand-off distance between the nozzle and the impingement surface, normalised by the nozzle diameter, z/D. A pressure transducer located in the plenum chamber of the nozzle allows for the measurement of the NPR, while an adjustable aluminum plate mounted downstream of the jet exit provides the impingement surface.

Schlieren imaging is a well established line-of-sight technique for the visualisation of the density gradients. Essentially, the density gradient is integrated along the line-of-sight, which allows the observation of strong dominant features above the mean density variation. In a classical Schlieren system such as the one here, density gradients can only be observed in a single direction (i.e. $d\rho/dx$, $d\rho/dr$) depending on the orientation of the knife-edge. Schlieren has a high sensitivity, which makes it particularly suitable for the present work to capture small scale structures of the impinging jet including Mach and acoustic waves and small vortical structures. For the interested reader, a more comprehensive description of the Schlieren technique is given in Settles (2001).
For the current experiments a Toepler Z-type Schlieren system is used and shown in Figure 1. The setup consist of two field mirrors with an effective focal length of 2032*mm*, a knife-edge placed at the focal point of the second field mirror and a spherical lens ($f = 500mm$) to collimate the light into the recording media.

As stated earlier, the emphasis of the this work is to image the impinging jet structure with a high spatial resolution. For this purpose, Schlieren images are recorded with a PCO Dimax camera with an array size of $2016 \times 2016\text{pixel}^2$ operating at a maximum framerate of $1000 fps$. The high spatial resolution of this camera makes it ideal to capture the small scale structures, but comes at the costs of a relatively low framerate. This means that the motion and dynamics of the individual structures, which are typically of the order of several hundreds of *kHz* (Risborg et al., 2008; Henderson et al., 2005) are not resolved in time. Therefore the results presented in the following sections should be considered independent of each other.
In order to capture a continuous record of the Schlieren images, light illumination is provided by means of a pulsed high-power LED similar to that used previously by Willert et al. (2010). The high-power LED, a Phlatlight PT-120 (532*nm*) is operated in pulsed mode using a custom built driving circuit capable of producing μs light pules at *kHz* repetition (see Buchmann et al. (2011) for more details). By over-driving the LED with currents on the order of 200*A*, the LED emits up to 60*W* without suffering any noticeable damage. This is sufficient to perform reliable Schlieren images with light pulses of $2.6\mu s$ duration at $1000 fps$.

3. RESULTS

Results presented in the following section are recorded using the above high spatial resolution Schlieren system to image the impinging supersonic jet at a $NPR = 3.2$ and a stand-off distance of $z/D = 4$.

3.1 VisualiSation of the Instability Mechanism

Figure 2 shows a series of instantaneous high-resolution Schlieren images of the key stages in the closed-loop instability

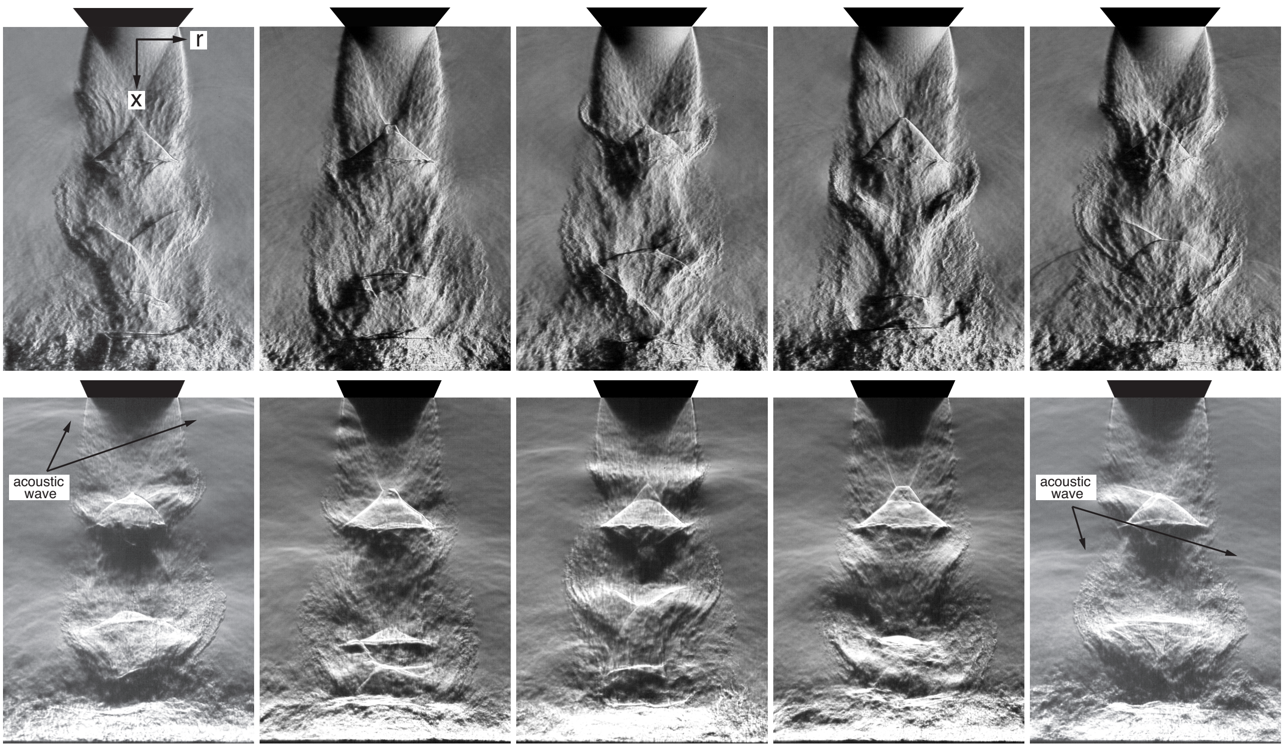

(a) (b) (c) (d) (e)

Figure 2: Sequence of instantaneous high-resolution Schlieren images of $d\rho/dr$ (top) and $d\rho/dx$ (bottom) representing the different stages of the acoustic feedback mechanism for $z/D = 4$, NPR=3.2 (flow from top to bottom)

mechanism, mentioned before, visualised by both $d\rho/dr$ (top) and $d\rho/dx$ (bottom). The images represent a single cycle, but are not taken from a single time-resolved sequence. Information pertaining to the temporal evolution of the underexpanded impinging jet is obtained from time-resolved visualisations presented previously by (Risborg et al., 2008). The spatial resolution of these temporally resolved visualisations is however insufficient to resolve the small, low amplitude vortices in the initial stage of the instability process. Figure 2(a) shows the upstream traveling acoustic wave prior to reaching the nozzle exit, which upon arrival causes a perturbation of the shear-layer clearly seen for $d\rho/dx$ in Figure 2(b). Following the initial disturbance the instability grows into a large-scale coherent structure that travels downstream towards the impingement surface as seen in Figure 2(c-d). As the large-scale structures pass over the shock cells within the jet, they induce significant fluctuating motion within the jet. This motion then generates a fluctuation in the wall jet, which in turn produces a sound wave (Fig. 2(e)), that travels back upstream to close the feedback loop.

A more detailed visualisation of the shear-layer instability is presented in Figure 3. The arrival of the acoustics wave at the nozzle lip (Fig. 3(a)) causes what is known as a sinusoidal-like disturbance of the shear-layer, which can clearly be seen in Figure 3(b). Through merging of the smaller high frequency vortices this instability evolves into a large low frequency structure, which becomes a rotational fluid packet due to the shear between the jet core and the quiescent ambient fluid (Fig. 3(c)). Subsequently, the initial disturbance grows in to a large-scale coherent structure, which exhibits characteristics of a Kelvin-Helmholtz vortex. As the structure convects downstream and increases in size it significantly penetrates into both the ambient fluid and the jet core (Fig. 3(d-e)) before reaching the impingement surface (not shown here).

3.2 Two-Point-Correlations

In order to further investigate the spatial extent of the instability feedback mechanisms, two-point-correlations of the axial density gradient $d\rho/dx$ are considered in the following. The two-point-correlation $R(\triangle x, \triangle r)$ is defined as following:

$$R(\triangle x, \triangle r) = \frac{\langle I(x_o, r_o) \cdot I(x_o + \triangle x, r_o + \triangle r)\rangle}{\sigma_{I_{x_o, r_o}} \sigma_{I_{x_o+\triangle x, r_o+\triangle r}}} \qquad (1)$$

where I is the fluctuating image intensity of the instantaneous Schlieren images $d\rho/dx$. The two-point-correlation is evaluated between the image intensities at a reference point (x_o, r_o) and the image intensities at $(x_o + \triangle x, r_o + \triangle r)$, ensemble averaged over more than 6000 instantaneous recordings and normalised by the sample variance. The spatial two-point-correlations are used to identify the extent over which the observed flow structures are correlated in space by roughly knowing their location in space and placing the reference point (x_o, r_o) at these locations.

Figure 4 shows the two-point-correlation for a point located just outside the nozzle and along the jet centerline. The correlation map shows a spatially periodic structure, which roughly correlates with the periodic shock structure observed in Figure 2(c). Around the fix-point (i.e. near-field), positive and negative correlations extend radially indicating a strong correlation with the surrounding acoustic waves. In the far-field, this correlation is weaker due to the higher fluctuations of the jet in this region that are caused by the passing and impinging large scale structures.

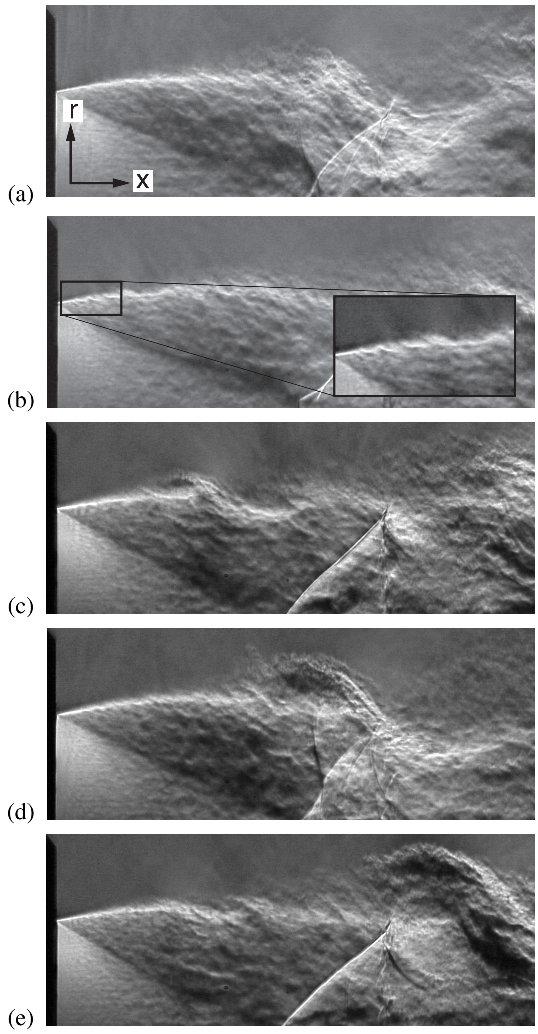

Figure 3: Detailed Schlieren visualisation of $d\rho/dx$ of the shear layer instability and its evolution into a large-scale coherent structure for $z/D = 4$, NPR=3.2 (flow from left to right)

Correlations in the shear-layer are shown in Figure 4(b-d), where the fixed point is placed at locations roughly corresponding to he phenomena observed in Figure 3(c-e). At the early development of the Kelvin-Helmholtz like instability the spatial correlations are only local and very confined in axial direction with little to no correlation with the acoustic field (Fig. 4(b)). As the instability proceeds and larger scale structures develop the correlation in downstream direction increases, while upstream events remain relatively uncorrelated (Fig. 4(c)). This may suggest that the instability created by the acoustic wave precedes the convecting vortex, which forms at the tail of the perturbation rather than at its leading edge. Further downstream as the coherent vortex impinges at the surface, correlations with the surrounding acoustic field become stronger again due the formation of new acoustic waves during the impingement event.

4. DISCUSSION AND CONCLUSIONS

This work has presented high spatial resolution Schlieren images of the instantaneous density gradients $d\rho/dx$ and $d\rho/dr$ in a supersonic underexpanded jet impinging on a flat plate. Although not time-resolved, the current result clearly reveal the

cyclic nature of the impingement process and provide a detailed visualisation of the closed loop instability mechanisms that drive the shear-layer instabilities through the interaction with the acoustic field. These instabilities cause the formation of large scale Kelvin-Helmholtz like structures in the shear-layer, which impart significant fluctuation into the jet core as they travel downstream to impinge on the surface where they set-off new acoustic waves. The correlation between the shear layer instabilities, the formation of large scale structure and the acoustic field is further evidenced by considering two-point-correlations of the axial density gradient $d\rho/dx$.
Besides the shear-layer instabilities observed herein, further instability modes relating to the shock structure inside the jet core exist. These include helical and semi-helical instabilities as well as axial pulsing, flapping and collapsing instabilities of the primary and secondary (or intermittent) Mach discs seen in Figure 2. These type of instabilities have not been considered here, but are the subject of previous investigations (Risborg et al., 2008). A time-resolved visualisation (both Schlieren and Shadowgraphy) of the some of these instabilities may be viewed online on http://media.efluids.com/galleries/compressible.

With regard to the cold spray coating process, the current results undoubtedly reveal the complex fluid dynamic nature of such industrial processes. It is likely that the trajectories of individual coating particle will be affected by the interaction of the particle with the complex flow field, making it difficult to predict their exact path, impingement velocity and impingement angle. Hence, the successful injection of the solid particle, their targeting and operation of the cold spray process strongly depends on the exact nature of underlying flow field, which will be determined by the operational conditions such as NPR and z/D.

Lastly, it should be mentioned that the high-power LED illumination used in this study is particularly well suited for the relatively low framerate (i.e. $1000 fps$) of the high-resolution CCD camera. Recording a continuous image sequence at such low framerates requires pulse durations on the order of only a few μs, which is much shorter than the flash durations of xenon flash lamps traditionally used in Schlieren and Shadowgraphy. The high repeatability of the LED pulses (see Buchmann et al. (2011)) also provides an even illumination and high image contrast, which renders image pre-processing unnecessary and allows further analysis of this high-resolution data.

ACKNOWLEDGMENTS

The support of the Australian Research Council through a Discovery Research Grant is greatly acknowledged.

REFERENCES

Buchmann, N., Willert, C., and Soria, J. (2011). Tomographic particle image velocimetry using pulsed, high power led volume illumination. In *8th International Symposium on Particle Image Velocimetry, Kobe, Japan*.

Carling, J. C. and Hunt, B. L. (1977). The near wall of a normally impinging uniform axisymmetric supersonic jet. *Journal of Fluid Mechanics*, 66(1):159–176.

Donaldson, C. D. and Snedeker, R. S. (1971). A study of free jet impingement. part 1. mean properties of free and impinging jets. *Journal of Fluid Mechanics*, 45(2):281–319.

Henderson, B., Bridges, J., and Wernet, M. (2005). An experimental study of the oscillatory flow structure of tone-producing supersonic impinging jets. *Journal of Fluid Mechanics*, 542(115-137).

Krothapalli, A., Rajkuperan, E., Alvi, F., and Lourenco, L. (1999). Flow field and noise characteristics of a supersonic impinging jet. *Journal of Fluid Mechanics*, 392(155-181).

Risborg, A., D., M., D., H., and Soria, J. (2008). Instabilities in underexpanding impinging jets. In *Fitfth Australian Conference on Laser Diagnostics in Fluid Mechanics and Combustion, Perth, Australia*.

Settles, G. (2001). *Schlieren and Shadowgraph Techniques. Experimental Fluid Mechanics*. Springer-Verlag.

Willert, C., Mitchell, D., and Soria, J. (2010). Megahertz schlieren imaging of shock structure and sound waves in under-expanded, impinging jets. In *arXiv physics.flu-dyn (2010). URL http://arxiv.org/abs/1010.3186v1*.

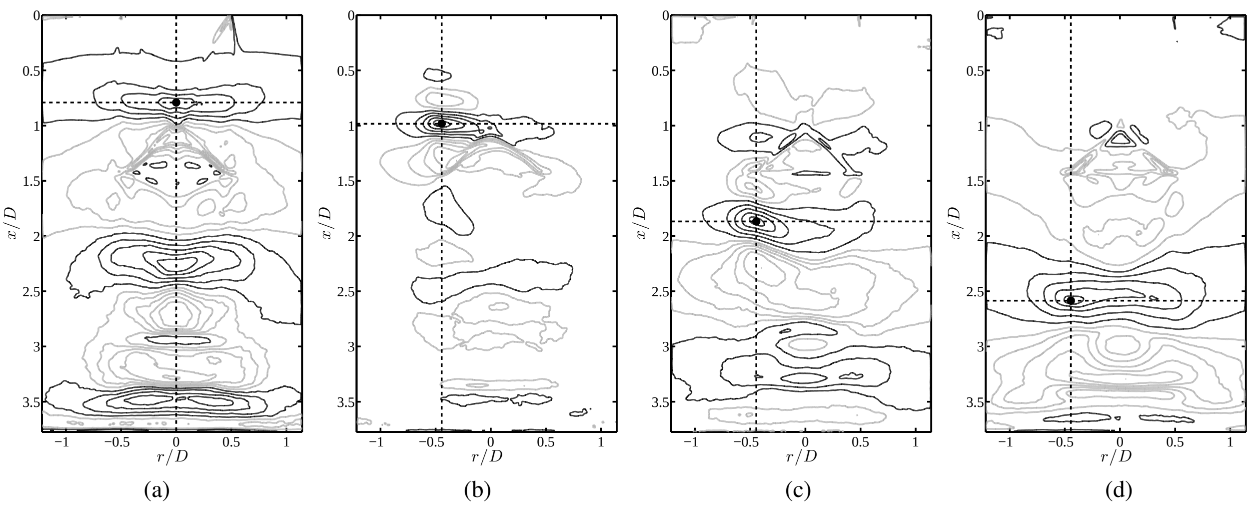

Figure 4: Two-point correlation of $d\rho/dx$ for $z/D = 4$, NPR = 3.2. Positive (—black), negative (—gray), reference point (•). Contour levels are drawn for the interval [-1:1] in increments of 0.15.